

Preparation and oxygen sensing properties of a sol–gel derived thin film based on a covalently grafted ruthenium(II) complex

Haoran Zhang^{a,b}, Bin Li^{a,*}, Bingfu Lei^a, Wenlian Li^a, Shaozhe Lu^a

^a Key Laboratory of Excited State Processes, Changchun Institute of Optics Fine Mechanics and Physics, Graduate School of the Chinese Academy of Sciences, Chinese Academy of Sciences, Changchun 130033, PR China

^b Faculty of Chemistry, Northeast Normal University, Changchun 130024, PR China

Received 2 July 2006; received in revised form 15 September 2006; accepted 19 September 2006

Available online 17 October 2006

Abstract

The preparation and properties of luminescent oxygen sensing materials based on a sol–gel derived thin film containing covalently grafted Ru(bpy)₃²⁺ fragments are described in this article. The 2,2'-bipyridyl covalently grafted to 3-aminopropyltriethoxysilane through Si–CH₂ covalent bonds was used as not only one of the sol–gel precursors but also the second ligand of Ru(bpy)₂Cl₂·2H₂O complex to prepare the sol–gel derived silicates for oxygen sensors. The luminescence of covalently grafted Ru(II) within the thin film can be extremely quenched by oxygen with good sensitivity ($I_0/I_{100} = 4.3$) and rapid response time (7 s), which suggests that the covalently grafting strategy presented in this article can be used for developing oxygen sensors. Furthermore, the thin film possesses the distinct advantages over those obtained by the physically entrapped method due to the Si–CH₂ covalent bonds, including greatly minimized dye leaching effect, faster detection and simplified linear Stern–Volmer plot. © 2006 Elsevier B.V. All rights reserved.

Keywords: Oxygen sensor; Ruthenium complex; Sol–gel method; Covalent grafting

1. Introduction

Life on earth relies on the presence of oxygen (O₂) and other gases in the atmosphere. The determination of O₂ concentration is important as O₂ is often involved in many chemical and biochemical reactions as reactants or products. Traditionally, O₂ is quantified by using a Clark-type amperometric electrode, which is based on the electroreduction of O₂ on a polarized cathode. In recent years, optical oxygen sensors are more attractive than conventional amperometric devices due to the following advantages: faster response time, high sensitivity and selectivity, no O₂ consumption, no poison and no requirement for a reference electrode [1–10]. The optical oxygen sensors mainly operate on the principle of oxygen quenching of dye molecules, which have been entrapped into a porous support matrix. The ruthenium(II) polypyridyl complexes are one of the most widely used oxygen-sensitive dyes because of their efficient quenching by molecular O₂, relatively long fluorescence lifetime determined

by the metal-to-ligand charge-transfer (MLCT) excited state, fast response time, strong visible absorption, large Stokes shift and high photochemical stability [6,7,9,11–18]. The sol–gel approach is an efficient immobilization technique for oxygen sensors based on ruthenium complexes due to its many desirable properties such as high thermal stability, good photostability and optical transparency in the visible light region [7,9,10,19–21]. Unfortunately, there are significant drawbacks when using these systems for oxygen sensors because only weak physical interactions exist between the dopants and the matrix, including inhomogeneous distribution of both organic/inorganic components, leaching of dopants, and poor flexibility [10,18–20,22]. In order to overcome the above-mentioned drawbacks, here we present a strategy to prepare a novel sol–gel derived oxygen sensing thin film based on covalently grafting the Ru(II) complex to the backbone of silica networks via Si–CH₂ covalent bonds. The luminescent and oxygen-sensing properties were systematically investigated. The typical sensitivity of the obtained film defined by I_0/I_{100} is 4.3 where I_0 and I_{100} denote the fluorescence intensities under 100% nitrogen and 100% oxygen condition, respectively. The response time t_Q and recovery time t_R are 7 and 23 s, respectively, which indicates that the thin film obtained

* Corresponding author. Fax: +86 431 6176935.
E-mail address: lib020@ciomp.ac.cn (B. Li).

in our present work meet the requirements of an oxygen sensor. Detection of dissolved oxygen can be expected because of the greatly improved anti-leaching, sensitivity, and stability of this kind of covalently grafted thin films.

2. Experimental

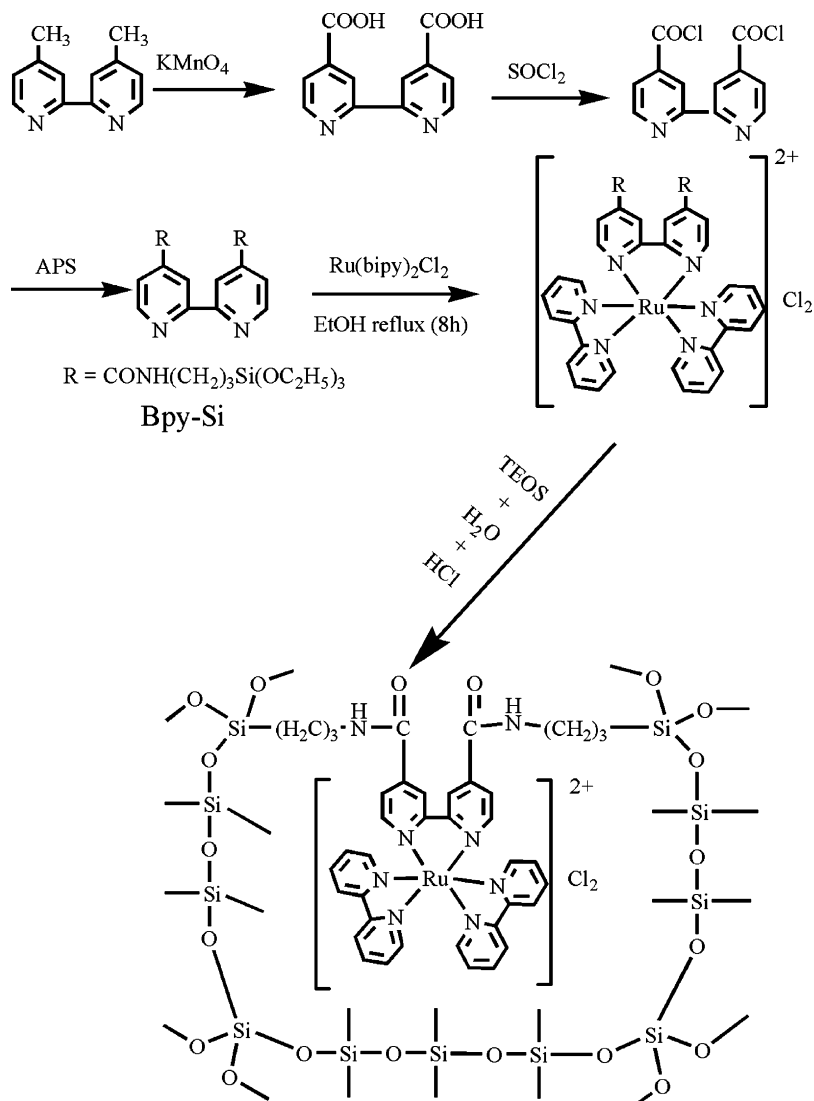
2.1. Chemical reagents

4,4'-Dimethyl-2,2'-bipyridyl and anhydrous RuCl_3 (99.99%) along with the 3-aminopropyltriethoxysilane (APS) were obtained from Aldrich (Milwaukee, WI, USA) and were used without further purification. Tetraethoxysilane (TEOS) and EtOH were purchased from Tianjin Chemicals Co. Concentrated HCl and thionyl chloride (SOCl_2 , A.R.) were obtained from Shanghai Chemical Co. SOCl_2 was used after distillation in vacuo. The complex bis(2,2'-bipyridyl)ruthenium(II) chloride dihydrate, $\text{Ru}(\text{bpy})_2\text{Cl}_2 \cdot 2\text{H}_2\text{O}$, was synthesized and purified as

described in the literature [23]. The water used in our work is de-ionized.

2.2. Sample preparation

The ligand (denoted as Bpy-Si, as shown in Scheme 1) was prepared using 2,2'-bipyridine-4,4'-dicarboxylic acid and APS as the starting materials. The synthesis of 2,2'-bipyridine-4,4'-dicarboxylic acid was performed by oxidation of 4,4'-dimethyl-2,2'-bipyridine by reflux in a potassium permanganate aqueous solution as described in detail in Ref. [23]. The detailed synthetic procedure of Bpy-Si has been reported elsewhere [24,25] and can be briefed as follows: 2,2'-bipyridine-4,4'-dicarboxylic acid (0.49 g; 2.00 mmol) was dissolved in excess distilled SOCl_2 (8 mL) and refluxed for 4 h. The excess SOCl_2 was eliminated by evaporation from the yellow solution, and the residual was reacted with APS under nitrogen for 4 h at room temperature in the presence of excess pyridine and using



Scheme 1. Synthesis procedure of hydrolysable $\text{Ru}(\text{bpy})_2(\text{Bpy-Si})\text{Cl}_2$ complex and the predicted structure of the finally obtained oxygen sensing material.

diethyl ether as a solvent (40 mL). Pyridinium hydrochloride was filtered and evaporation of the residual organic solvent gave the alkoxysilane-modified bipyridine ligand Bpy-Si.

To obtain the hydrolysable complex $\text{Ru}(\text{bpy})_2(\text{Bpy-Si})\text{Cl}_2$, a mixture of $\text{Ru}(\text{bpy})_2\text{Cl}_2$ and Bpy-Si in anhydrous ethanol was refluxed for 8 h in nitrogen atmosphere to give a transparent deep red solution, indicating that the complexation reaction between Bpy-Si and $\text{Ru}(\text{bpy})_2\text{Cl}_2$ had finished. The molar ratio of Bpy-Si to $\text{Ru}(\text{bpy})_2\text{Cl}_2$ was 1.02:1. Finally the ethanol was rotary evaporated off and the residue was dried in vacuo without any further purification.

The sol–gel derived thin film for an oxygen sensor was prepared using $\text{Ru}(\text{bpy})_2(\text{Bpy-Si})\text{Cl}_2$ as one of the precursor, which reacted with TEOS by hydrolysis and condensation. The following particular procedure was chosen because it is representative of TEOS-based xerogels reported in literatures [6,7,13,19,24–27]. A starting solution was prepared by dissolving the complex $\text{Ru}(\text{bpy})_2(\text{Bpy-Si})\text{Cl}_2$ (14.2 mg) in ethanol (1.5 mL) in a plastic vial and stirred for 5 min, and then 5 mL of TEOS was added for another 5 min stirring, followed by H_2O and HCl addition. A minimal amount of tetrahydrofuran was added to the solution to solubilize the Ru(II) complex in the sol more efficiently. The final molar ratio of constituents was $\text{TEOS}:\text{H}_2\text{O}:\text{C}_2\text{H}_5\text{OH}:\text{HCl}=1:4:4:0.01$. The concentration of $\text{Ru}(\text{bpy})_2(\text{Bpy-Si})\text{Cl}_2$ in the final sol was 2×10^{-3} M. The solution was kept stirring at room temperature for 4 h prior to the dip-coating of the sol onto a freshly cleaned sodalime silicate glass substrate. Each side of the glass substrate was firstly cleaned by soaking in 1 M NaOH for 30 min and washing 10 times with deionized water and EtOH, finally dried under ambient conditions. The withdrawing rate was set as 5 cm/min to give a wet gel film. The as-synthesized thin film was dried under ambient conditions in the dark for at least 2 weeks before any measurement. Finally, optically transparent crack-free thin film was obtained and the adhesion of the sol to the substrate was found to be excellent.

2.3. Instruments and measurements

The infrared absorption spectra were measured in the region of $400\text{--}4000\text{ cm}^{-1}$ by a Fourier transform infrared (FTIR) spectrophotometer (Model Perkin-Elmer Model 580B) with a resolution of $\pm 4\text{ cm}^{-1}$ using the KBr pellet technique. The UV–vis electronic absorption measurements of the final products were performed with a Shimadzu UV-3000 spectrophotometer with a resolution of $\pm 1\text{ nm}$.

The photoluminescence (PL) spectra of the thin films prepared were obtained in aerated environments by a Hitachi F-4500 fluorescence spectrophotometer equipped with a monochromator (resolution: 0.2 nm) and a 150 W Xe lamp as the excitation source. Suitable filters were used to correct for the baseline shift due to any stray light.

The oxygen sensing properties of our present sol–gel derived thin film were discussed based on the fluorescence intensity quenching instead of the excited state lifetime because it is hard to obtain the precise excited state lifetime value with a conventional flashlamp-based time-correlated photo-counting system.

The excitation wavelength of all samples was 475 nm. The excitation spectrum was obtained monitoring at the wavelength of peak emission (625 nm).

For the Stern–Volmer plot measurement, oxygen and nitrogen were mixed at different concentrations via gas flow controllers and passed directly to the sealed gas chamber. We typically allowed 1 min between changes in the N_2/O_2 concentration to ensure that a new equilibrium point had been established. Equilibrium was evident when the luminescence intensity remained constant ($\pm 2\%$). The O_2 concentrations were accurate to $\pm 1\%$ [28]. The sensor response curves were obtained using the same method.

In the measurement of fluorescence lifetime of the Ru complex incorporated within the thin film, a 266 nm light generated from the Fourth-Harmonic-Generator pumped by a pulsed Nd:YAG laser was used as an excitation source. The Nd:YAG laser was with a line width of 1.0 cm^{-1} , pulse duration of 10 ns and repetition frequency of 10 Hz. A Rhodamine 6G dye pumped by the same Nd:YAG laser was used as the frequency-selective excitation source. All measurements were performed at room temperature.

3. Results and discussion

By using the double-role Bpy-Si compound, as a second ligand for complex $\text{Ru}(\text{bpy})_2\text{Cl}_2$ and as a sol–gel precursor, we have succeeded in covalently grafting the complex $\text{Ru}(\text{bpy})_3\text{Cl}_2$ to the functionalised silicates produced via a sol–gel approach for oxygen sensors. The synthesis procedure of this material is outlined in Scheme 1.

The presence of organic ligands covalently bonded to the network of the modified silicate is characterized by FTIR. The FTIR spectra of hydrolysable $\text{Ru}(\text{bpy})_2(\text{Bpy-Si})\text{Cl}_2$ complex (a) and the final oxygen sensing material (b) are shown in Fig. 1. In Fig. 1a, the spectrum of $\text{Ru}(\text{bpy})_2(\text{Bpy-Si})\text{Cl}_2$ is dominated by $\nu(\text{C-Si}, 1208\text{ cm}^{-1})$ and $\nu(\text{Si-O}, 1079\text{ cm}^{-1})$

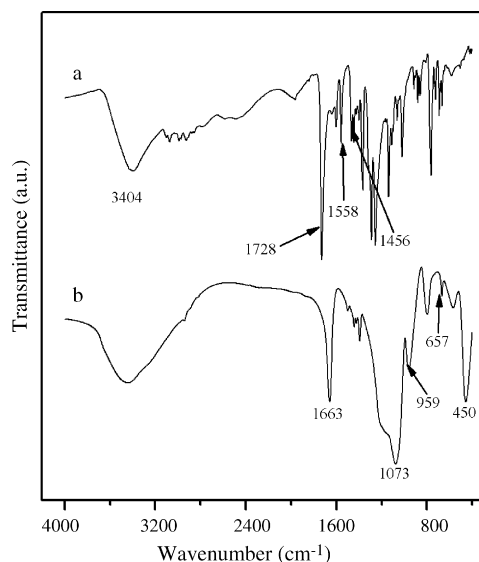


Fig. 1. FTIR spectra of (a) hydrolysable $\text{Ru}(\text{bpy})_2(\text{Bpy-Si})\text{Cl}_2$ complex and (b) the finally obtained oxygen sensing material.

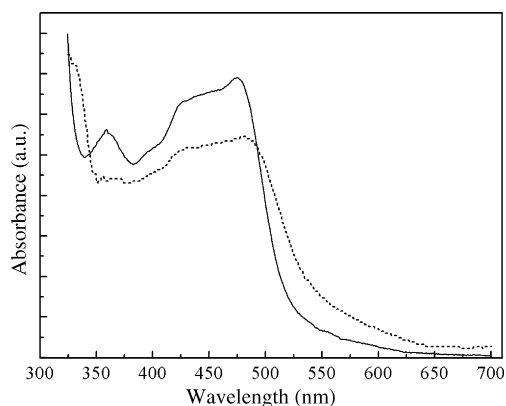


Fig. 2. Optical absorption spectra of $\text{Ru}(\text{bpy})_2(\text{Bpy-Si})\text{Cl}_2$ complex in ethanol (solid line) and the final oxygen sensing material (dash line).

absorption bands, which are the characteristics of trialkoxysilyl functions [29]. Furthermore, the bending vibration of Si–O at 462 cm^{-1} from APS is obvious in Fig. 1a, indicating that the APS has been successfully grafted onto 2,2'-bipyridine [24]. In panel b of Fig. 1, the formation of the Si–O–Si framework is evidenced by the bands located at 1088 and 1080 cm^{-1} (ν_{as} , Si–O), 802 and 799 cm^{-1} (ν_{s} , Si–O), and 456 and 462 cm^{-1} (δ , Si–O–Si) (ν represents stretching, δ in-plane bending, s symmetric, and as asymmetric vibrations) [24]. The peaks at 1656 and 1636 cm^{-1} , originating from the CONH group of Bpy-Si, can also be observed in the as-synthesized material, which is consistent with the fact that the Bpy-Si group in the framework remains intact after the hydrolysis/condensation reaction. Furthermore, the broad absorption band at 1120 – 1000 cm^{-1} corresponding to the $\nu(\text{Si-O-Si})$, as shown in Fig. 1b, indicates the formation of siloxane network. The introduction of TEOS and water to the $\text{Ru}(\text{bpy})_2(\text{Bpy-Si})\text{Cl}_2$ results in the changes in the IR spectra (as shown in Fig. 1a and b) due to the hydrolysis/condensation of TEOS and $\text{Ru}(\text{bpy})_2(\text{Bpy-Si})\text{Cl}_2$. The remained $\nu(\text{Si-C})$ vibration located at 1208 cm^{-1} indicates that no (Si–CH₂) bond cleavage occurs during the hydrolysis/condensation reactions.

Fig. 2 represents the optical absorption spectra of $\text{Ru}(\text{bpy})_2(\text{Bpy-Si})\text{Cl}_2$ complex in ethanol and the final oxygen sensor material. Both absorption spectra show an intense band at 475 nm which can be assigned to the MLCT ($t_{2g}(\text{Ru}) \rightarrow \pi^*(\text{L})$) transition, and a smaller band at 360 nm originated from metal centered (MC) d–d transition [30–33]. The shoulder at 427 nm is attributed to the splitting of the first excited state energy level into two separate levels caused by the trigonal symmetry of the complex [31–34]. As shown in Fig. 2, the absorption features of $\text{Ru}(\text{bpy})_2(\text{Bpy-Si})\text{Cl}_2$ complex entrapped in the final oxygen sensor material are not significantly changed from that observed in ethanol, indicating that there is no interaction between the complex and the sol–gel matrix in the energetically ground state.

Fig. 3 shows the fluorescence emission spectra of $\text{Ru}(\text{bpy})_2(\text{Bpy-Si})\text{Cl}_2$ complex dissolved in ethanol and the final thin film oxygen sensor. We can see that the emission spectra show a broad band ranging from 550 to 750 nm . The broad-band fluorescence emission arises from ligand to metal charge-transfer excited state where the emitting state is derived from a configuration involving promoting a metal d electron to a ligand

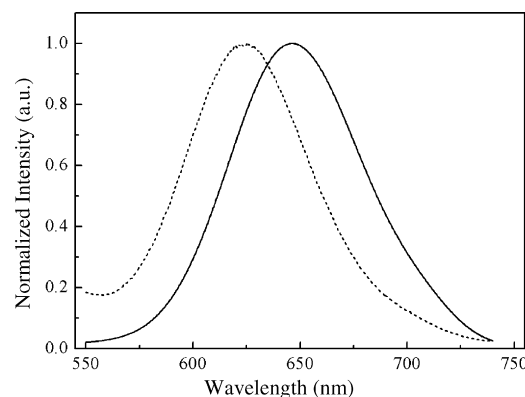


Fig. 3. Emission spectra of $\text{Ru}(\text{bpy})_2(\text{Bpy-Si})\text{Cl}_2$ complex dissolved in ethanol (solid line) and the final thin film oxygen sensing material (dash line).

π^* antibonding orbital [15]. The emission maximum wavelength shows a blue shift of 21 nm from 646 to 625 nm when the complex is immobilized within the sol–gel derived thin film. This is probably caused by the change of the MLCT excited state within the hybrid thin film during the formation of Si–O network structure. Such a blue shift can be explained on the basis of the suppression of the vibrational deactivation and the restriction on the mobility of the Ru(II) complex in an excited-state due to the rigidity of silica matrix [16,18,35–37].

Optical sensors based on the luminescence quenching are examined by the Stern–Volmer equation. In homogeneous media with a single-exponential decay, the intensity and lifetime forms of the Stern–Volmer equation with dynamic quenching are as follows:

$$\frac{I_0}{I} = \frac{\tau_0}{\tau} = 1 + K_{\text{SV}}[\text{O}_2] = 1 + \kappa\tau_0[\text{O}_2] \quad (1)$$

where I and τ are the fluorescence intensity and excited-state lifetime of the luminophore, respectively, the subscript 0 denotes the absence of oxygen, K_{SV} is the Stern–Volmer constant, κ is the bimolecular rate constant describing the efficiency of the collisional encounters between the luminophore and the quencher, and $[\text{O}_2]$ is the oxygen concentration. A plot of I_0/I or τ_0/τ versus oxygen concentration should give a straight-line relationship with a slope K_{SV} , and an intercept of 1 on the y-axis [9].

The luminescence of most Ru(II)-bipyridine complexes could be quenched effectively by molecular oxygen. The room temperature emission spectra, which are recorded for a typical covalently grafted $\text{Ru}(\text{bpy})_2(\text{Bpy-Si})\text{Cl}_2$ thin film oxygen sensor under different concentrations of oxygen, are presented in Fig. 4. The position and shape of the 625 nm MLCT emission from $\text{Ru}(\text{bpy})_2(\text{Bpy-Si})\text{Cl}_2$ is constant under different oxygen concentrations. However, the relative intensity decreases markedly with increasing the oxygen concentration. The relative luminescent intensities of the $\text{Ru}(\text{bpy})_2(\text{Bpy-Si})\text{Cl}_2$ -doped thin film oxygen sensor decrease by 77.9% upon changing from pure nitrogen to pure oxygen.

Fig. 5 presents the Stern–Volmer plot for a typical covalently grafted $\text{Ru}(\text{bpy})_2(\text{Bpy-Si})\text{Cl}_2$ thin film oxygen sensor. The estimated uncertainties on the I_0/I are 1 – 4% based on the precision of the individual intensity measurements. For com-

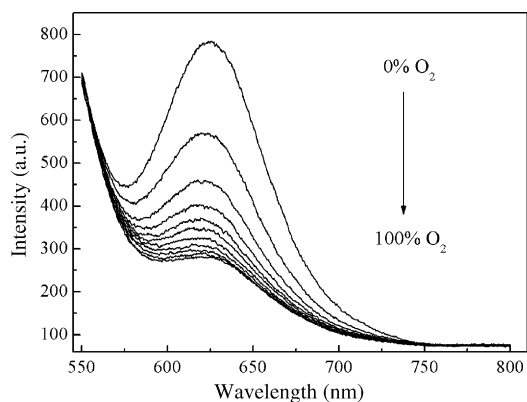


Fig. 4. Emission spectra of a typical covalently grafted $\text{Ru}(\text{bpy})_2(\text{Bpy-Si})\text{Cl}_2$ thin film oxygen sensor subjected to different oxygen concentrations.

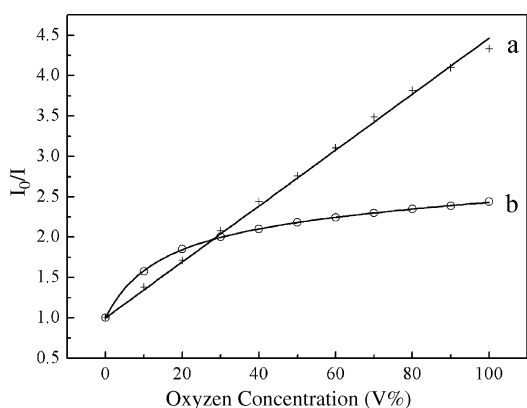


Fig. 5. Typical fluorescence intensity-based Stern–Volmer plots for the oxygen sensors: (a) covalently grafted $\text{Ru}(\text{bpy})_2(\text{Bpy-Si})\text{Cl}_2$ thin film and (b) physically incorporated $\text{Ru}(\text{bpy})_3\text{Cl}_2$ thin film. The solid lines represent the best fit to a Demas model (the physically incorporated sample, plot b) or Stern–Volmer model (plot a).

parative purpose, the Stern–Volmer plot of an oxygen sensor, in which $\text{Ru}(\text{bpy})_3\text{Cl}_2$ was physically incorporated into the sol–gel derived matrix by a conventional method, is also given in Fig. 5. As shown in Fig. 5, the Stern–Volmer plot of the covalently grafted sample shows good linearity; however, the physically incorporated sample without Si–CH₂ covalent bonds exhibits obvious downward curvature. We attribute the good linear Stern–Volmer plot of the covalently grafted sample to the Si–CH₂ covalent bonds that act as a contributor to the network of the modified silicate matrix resulting in the uniform distribution of luminophore. The non-linearity of the physically incorpo-

rated sample is associated with the luminophore molecules being distributed simultaneously between two or more sites within the sol–gel derived silicate in which one site is more heavily quenched than the other [15,38–40]. Consequently, the different microheterogeneous sites exhibit different quenching constants K_{SV} and unquenched lifetime τ_0 values. In this case, the single-exponential decay Stern–Volmer equation (as shown in Eq. (1)) cannot be used to describe the oxygen sensing data. In this kind of microheterogeneous solid-based oxygen sensor, a two-site model has been found to have excellent ability to fit the experiment data [7,9,22]. In this model, the straight-line intensity-based Stern–Volmer equation then becomes.

$$\frac{I_0}{I} = \frac{1}{\frac{f_{01}}{1+K_{\text{SV}1}[\text{O}_2]} + \frac{f_{02}}{1+K_{\text{SV}2}[\text{O}_2]}} \quad (2)$$

where f_{0i} valuables are the fraction of each of the two sites contributing to the unquenched intensities and the $K_{\text{SV}i}$ values are the associated Stern–Volmer quenching constants for the two sites. The fitting parameters of Fig. 5 are tabulated in Table 1.

For oxygen sensors, short response and recovery time are very important when exposed to practical application. Generally, 95% response time, i.e., $t_{\downarrow}(95\%, \text{N}_2 \rightarrow \text{O}_2)$, is defined as the time required for the luminescent intensity to decrease by 95% on changing from 100% N_2 to 100% O_2 . Similarly, 95% recovery time, i.e., $t_{\uparrow}(95\%, \text{O}_2 \rightarrow \text{N}_2)$, means the time required for the luminescence intensity to reach the 95% of its initial value recorded under 100% N_2 on changing from 100% O_2 to 100% N_2 [5]. Fig. 6 shows the typical dynamic response of the covalently grafted thin film oxygen sensor upon repeated exposure to oxygen/nitrogen cycles in the gas phase. Upon changing to pure O_2 , the emission intensity drops very quickly, while upon changing to pure N_2 , the emission intensity increases and recovers to its initial value. From this time dependent measurement we can see that the sensor response is stable and reversible. The evaluated time for the change in the PL signal to 95% of the final value is found to be about 23 s on going from 100% O_2 to 100% N_2 and about 7 s on going from 100% N_2 to 100% O_2 . This result shows that the response time is shorter than the recover time distinctly, similar to the results obtained for Pt-OEP in a polymer medium [41], and this difference can be explained by the stronger adsorption of oxygen than that of nitrogen on the silica surface [18].

Fig. 7 shows the typical excited-state intensity decay profile for a randomly selected covalently grafted $\text{Ru}(\text{bpy})_2(\text{Bpy-Si})\text{Cl}_2$ thin film measured in the ambient atmosphere. It is clear

Table 1
Intensity-based Stern–Volmer oxygen quenching fitting parameters for covalently grafted $\text{Ru}(\text{bpy})_2(\text{Bpy-Si})\text{Cl}_2$ thin film and physically incorporated $\text{Ru}(\text{bpy})_3\text{Cl}_2$ thin film^a

Samples	I_0/I_{100}	Stern–Volmer		Demas ^b			
		$K_{\text{SV}}([\text{O}_2]^{-1})$	r^2	$K_{\text{SV}1}([\text{O}_2]^{-1})$	$K_{\text{SV}2}([\text{O}_2]^{-1})$	f_{01}^c	r^2
Physically incorporated thin film	2.44			0.1660 (± 0.0055)	0.0010 (± 0.0001)	0.59 (± 0.01)	0.9998
Covalently grafted thin film	4.29	0.0347 (± 0.0003)	0.9975	0.0407 (± 0.0017)	0.0047 (± 0.0005)	0.94 (± 0.01)	0.9999

^a When an entry is not listed, the given model is the best given; Sample aged for 2 months.

^b Terms are from Eq. (2).

^c $f_{01} + f_{02} = 1$.

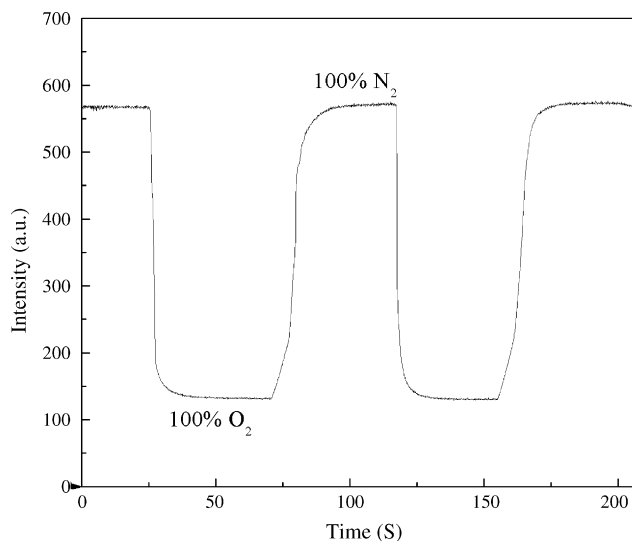


Fig. 6. Relative luminescence intensity of 625 nm emission as a function of time for a typical covalently grafted $\text{Ru}(\text{bpy})_2(\text{Bpy-Si})\text{Cl}_2$ thin film subjected to an atmosphere which was varied periodically between 100% N_2 and 100% O_2 .

that the final thin film luminescence exhibits an almost single exponential excited-state decay profile, confirming the fact that $\text{Ru}(\text{II})$ complex molecules within the modified silicate occupy the same microenvironment sites and the distribution is uniform and homogeneous. These results are similar to that previously reported by Bright et al. [7]. The result of the excited-state intensity decay profile is consistent with the Stern–Volmer plot (as shown in Fig. 5).

Dissolved oxygen sensing is of major importance in environmental, industrial and medical applications. One fundamental but crucial question that remains when this kind of covalently grafted oxygen sensor is used for the dissolved oxygen detection is whether the luminophore leaches into the liquid phase. For this consideration, complex-leaching experiment was performed by soaking the covalently grafted $\text{Ru}(\text{bpy})_2(\text{Bpy-Si})\text{Cl}_2$ thin film in water, DMF and ethanol at 60°C in a sealed cuvette under magnetic stirring and then dried at 100°C in vacuo, as described previously [27]. These results reveal that the covalently grafted oxygen sensor possesses greatly enhanced chemical durability in

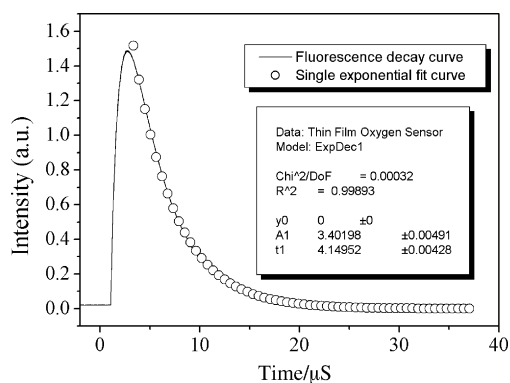


Fig. 7. Typical excited-state intensity decay profile for a randomly selected covalently grafted $\text{Ru}(\text{bpy})_2(\text{Bpy-Si})\text{Cl}_2$ thin film. The scatter line is the best fit to the experimental data using the single exponential decay model.

comparison with the physically incorporated thin film. The integrated fluorescence intensities of the unquenched MLCT emission of the covalently grafted sample after stirring in each solvent for 5 days were stable and no leaching effect was observed, while the integrated fluorescence of the physically incorporated sample dropped by 45%. This result reveals that the Si-CH_2 covalent bonds between the complex and the sol–gel matrix can effectively prevent the dopant leaching, which entirely agrees with the report by Li et al. [27]. The great minimization of the leaching is a crucial aspect for the dissolved oxygen sensor applications. Work is currently underway in our laboratory to fully characterize the dissolved oxygen sensing properties.

4. Conclusion

A covalent grafting strategy about preparation of optical sol–gel derived thin films for oxygen sensor material with high photochemical stability and good linearity Stern–Volmer plot was presented in this article. No leaching effect can be observed since these luminescence molecules were covalently grafted to the Si-O network; this properties make them show potential applications in monitoring the dissolved oxygen in liquid phase. The Si-CH_2 covalent bonds between the $\text{Ru}(\text{II})$ complex and the sol–gel derived modified silicate matrix as a network contributor result in enhanced anti-leaching, sensitivity, homogeneous distribution and linearity of the Stern–Volmer plot. This new kind of covalently grafted thin film can be further improved via changing the microstructure of the sensor support, and further work is in progress. Furthermore, the covalent grafting strategy reported in this article allows one to extend this method to prepare other organometallic complex doped devices with high performance.

Acknowledgments

The authors gratefully thank the financial supports of One Hundred Talents Project from Chinese Academy of Sciences, and the National Natural Science Foundations of China (Grant No. 20571071).

References

- [1] L. Huynh, Z. Wang, V. Stoeva, A. Lough, I. Manners, M.A. Winnik, Evaluation of phosphorescent Rhenium and Iridium complexes in polythionylphosphazene films for oxygen sensor applications, *Chem. Mater.* 17 (2005) 4765–4773.
- [2] M.E. Kose, A. Omar, C.a. Virgin, B.F. Carroll, K.S. Schanze, Principal component analysis calibration method for dual-luminophore oxygen and temperature sensor films: application to luminescence imaging, *Langmuir* 21 (2005) 9110–9120.
- [3] B.H. Han, I. Manners, M.A. Winnik, Oxygen sensors based on mesoporous silica particles on layer-by-layer self-assembled films, *Chem. Mater.* 17 (2005) 3160–3171.
- [4] M.E. Kose, B.F. Carroll, K.S. Schanze, Preparation and spectroscopic properties of multiluminophore luminescent oxygen and temperature sensor films, *Langmuir* 21 (2005) 9121–9129.
- [5] H. Zhang, Y. Sun, K. Ye, P. Zhang, Y. Wang, Oxygen sensing materials based on mesoporous silica MCM-41 and $\text{Pt}(\text{II})$ -porphyrin complexes, *J. Mater. Chem.* 15 (2005) 3181–3186.

- [6] R.M. Bukowski, R. Ciriminna, M. pagliaro, F.V. Bright, Photostability of luminescent ruthenium(II) complexes in polymers and in solution, *Anal. Chem.* 77 (2005) 2670–2677.
- [7] Y. Tang, E.C. Tehan, Z. Tao, F.V. Bright, Sol–gel-derived sensor materials that yield linear calibration plots, high sensitivity, and long-term stability, *Anal. Chem.* 75 (2003) 2407–2413.
- [8] M.C. DeRosa, P.J. Mosher, G.P.A. Yap, K.S. Focsaneanu, R.J. Crutchley, C.E.B. Evans, Synthesis, characterization, and evaluation of $[\text{Ir}(\text{ppy})_2(\text{vpy})\text{Cl}]$ as a polymer-bound oxygen sensor, *Inorg. Chem.* 42 (2003) 4864–4872.
- [9] M.T. Murtagh, M.R. Shahriari, M. Krihak, A study of the effects of organic modification and processing technique on the luminescence quenching behavior of sol–gel oxygen sensors based on a Ru(II) complex, *Chem. Mater.* 10 (1998) 3862–3869.
- [10] C. McDonagh, B.D. MacCraith, A.K. McEvoy, Tailoring of sol–gel films for optical sensing of oxygen in gas and aqueous phase, *Anal. Chem.* 70 (1998) 45–50.
- [11] K. Matsui, F. Momose, Luminescence properties of tris(2,2'-bipyridine)ruthenium(II) in sol–gel systems of SiO_2 , *Chem. Mater.* 9 (1997) 2588–2591.
- [12] D.S. Tyson, J. bialecki, F.N. Castellano, Ruthenium(II) complex with a notably long excited state lifetime, *Chem. Commun.* 23 (2000) 2355–2356.
- [13] C. McDonagh, P. Bowe, K. Mongey, B.D. MacCraith, Characterisation of porosity and sensor response times of sol–gel-derived thin films for oxygen sensor applications, *J. Non-Cryst. Solids* 306 (2002) 138–148.
- [14] K. Matsui, K. Sasaki, N. Takahashi, Luminescence of tris(2,2'-bipyridine)ruthenium(II) in sol–gel glasses, *Langmuir* 7 (1991) 2866–2868.
- [15] E.R. Carraway, J.N. Demas, B.A. DeGraff, J.R. Bacon, Photophysics and photochemistry of oxygen sensors based on luminescent transition-metal complexes, *Anal. Chem.* 63 (1991) 337–342.
- [16] P. Innocenzi, H. Kozuka, T. Yoko, Fluorescence properties of the $\text{Ru}(\text{bpy})_3^{2+}$ complex incorporated in sol–gel-derived silica coating films, *J. Phys. Chem. B* 101 (1997) 2285–2291.
- [17] M.M.F. Choi, D. Xiao, Single standard calibration for an optical oxygen sensor based on luminescence quenching of a ruthenium complex, *Anal. Chim. Acta* 403 (2000) 57–65.
- [18] X. Chen, Z. Zhong, Z. Lia, Y. Jiang, X. Wang, K. Wong, Characterization of ormosil film for dissolved oxygen-sensing, *Sens. Actuators B* 87 (2002) 233–238.
- [19] C. Malins, S. Fanni, H.G. Glever, J.G. Vos, B.D. MacCraith, The preparation of a sol–gel glass oxygen sensor incorporating a covalently bound fluorescent dye, *Anal. Commun.* 36 (1999) 3–4.
- [20] A.K. McEvoy, C.M. McDonagh, B.D. MacCraith, Dissolved oxygen sensor based on fluorescence quenching of oxygen-sensitive ruthenium complexes immobilized in sol–gel-derived porous silica coatings, *Analyst* 121 (1996) 785–788.
- [21] S.K. Lee, I. Okura, Optical sensor for oxygen using a porphyrin-doped sol–gel glass, *Analyst* 122 (1997) 81–84.
- [22] J.N. Demas, B.A. DeGraff, W. Xu, Modeling of luminescence quenching-based sensors: comparison of multisite and nonlinear gas solubility models, *Anal. Chem.* 67 (1995) 1377–1380.
- [23] G. Sprintschnik, H.W. Sprintschnik, P.P. Kirsch, D.G. Whitten, Preparation and photochemical reactivity of surfactant ruthenium(II) complexes in monolayer assemblies and at water–solid interfaces, *J. Am. Chem. Soc.* 99 (1977) 4947–4954.
- [24] H.R. Li, J. Lin, H.J. Zhang, H.C. Li, L.S. Fu, Q.G. Meng, Novel, covalently bonded hybrid materials of europium (terbium) complexes with silica, *Chem. Commun.* 13 (2001) 1212–1213.
- [25] H. Li, J. Yu, F. Liu, H. Zhang, L. Fu, Q. Meng, C. Peng, J. Lin, Preparation and luminescence properties of in situ formed lanthanide complexes covalently grafted to a silica network, *New J. Chem.* 28 (2004) 1137–1141.
- [26] R.T. Bailey, F.R. Cruickshank, G. Deans, R.N. Gillanders, M.C. Tedford, Characterization of a fluorescent sol–gel encapsulated erythrosin B dissolved oxygen sensor, *Anal. Chim. Acta* 487 (2003) 101–108.
- [27] H.R. Li, J. Lin, H.J. Zhang, L.S. Fu, Q.G. Meng, S.B. Wang, Preparation and luminescence properties of hybrid materials containing europium(III) complexes covalently bonded to a silica matrix, *Chem. Mater.* 14 (2002) 3651–3655.
- [28] R.A. Dunbar, J.D. Jordan, F.V. Bright, Development of chemical sensing platforms based on sol–gel-derived thin films: Origin of film age vs performance trade-offs, *Anal. Chem.* 68 (1996) 604–610.
- [29] C. Peng, H. Zhang, J. Yu, Q. Meng, L. Fu, H. Li, L. Sun, X. Guo, Synthesis, characterization, and luminescence properties of the ternary europium complex covalently bonded to mesoporous SBA-15, *J. Phys. Chem. B* 109 (2005) 15278–15287.
- [30] M.J. Cook, A.P. Lewis, G.S.G. McAuliffe, V. Skarda, A.J. Thomson, J.L. Glasper, D.J. Robbins, Luminescent metal complexes. Part 1. Tris-chelates of substituted 2,2-bipyridyls with ruthenium(II) as dyes for luminescent solar collectors, *J. Chem. Soc., Perkin Trans. 2* (1984) 1293–1301.
- [31] P. Belser, C. Daul, A. Von Zelewsky, On the assignment of the MLCT transition in the $\text{Ru}(\text{bpy})_3^{2+}$ complex ion, *Chem. Phys. Lett.* 79 (1981) 596–598.
- [32] J. Ferguson, F. Herren, A model for the interpretation of the electronic spectra of the complex-ion $\text{M}(\text{bpy})_3^{2+}$ ($\text{M} = \text{Fe}, \text{Ru}, \text{Os}$) in D_3 and D_2 sites, *Chem. Phys.* 76 (1983) 45–59.
- [33] E.M. Kober, T.J. Meyer, Concerning the absorption spectra of the ions $\text{M}(\text{bpy})_3^{2+}$ ($\text{M} = \text{Fe}, \text{Ru}, \text{Os}$; $\text{bpy} = 2,2'$ -bipyridine), *Inorg. Chem.* 21 (1982) 3967–3977.
- [34] A. Juris, V. Balzani, F. Barigelli, S. Campagna, P. Belser, A. von Zelewsky, Ru(II) polypyridine complexes: photophysics, photochemistry, electrochemistry, and chemiluminescence, *Coord. Chem. Rev.* 84 (1988) 85–277.
- [35] M. Wrighton, D.L. Morse, The nature of the lowest excited state in tricarbonylchloro-1,10-phenanthroline-ruthenium(I) and related complexes, *J. Am. Chem. Soc.* 96 (1974) 998–1003.
- [36] F.N. Castellano, T.A. Heimer, M.T. Tandhasetti, G.J. Meyer, Photophysical properties of ruthenium polypyridyl photonic SiO_2 gels, *Chem. Mater.* 6 (1994) 1041–1048.
- [37] P.J. Giordano, M.S. Wrighton, The nature of the lowest excited state in *fac*-tricarbonylhalobis(4-phenylpyridine)ruthenium(I) and *fac*-tricarbonylhalobis(4,4'-bipyridine)ruthenium(I): emissive organometallic complexes in fluid solution, *J. Am. Chem. Soc.* 101 (1979) 2888–2897.
- [38] J.R. Bacon, J.N. Demas, Determination of oxygen concentrations by luminescence quenching of a polymer-immobilized transition-metal complex, *Anal. Chem.* 59 (1987) 2780–2785.
- [39] I. Klimant, P. Belser, O.S. Wolfbeis, Novel metal-organic ruthenium(II) diimin complexes for use as longwave excitable luminescent oxygen probes, *Talanta* 41 (1994) 985–991.
- [40] L. Sacksteder, J.N. Demas, B.A. DeGraff, Design of oxygen sensors based on quenching of luminescent metal complexes: effect of ligand size on heterogeneity, *Anal. Chem.* 65 (1993) 3480–3483.
- [41] A. Mills, A. Lepre, Controlling the response characteristics of luminescent porphyrin plastic film sensors for oxygen, *Anal. Chem.* 69 (1997) 4653–4659.

Biographies

Haoran Zhang is a postgraduate student in the Faculty of Chemistry of Northeast Normal University (NNU) in China. She studies as an assistant graduate at the Key Laboratory of Excited State Processes of Changchun Institute of Optics Fine Mechanics and Physics (CIOMP) under the supervising of Prof. Bin LI since 2004. Her current research is the oxygen sensor based on fluorescence quenching of covalently grafted ruthenium complex within silica. She will receive her MSc degree in the coming year in inorganic chemistry from NNU.

Bin Li received his BSc in 1986 and MSc in 1991 in Inorganic Chemistry from NNU, and PhD in 1997 in Inorganic Chemistry from Changchun Institute of Applied Chemistry of Chinese Academy of Sciences (CAS), and then he became a postdoc at the State Key Laboratory of Inorganic Synthesis and Preparative Chemistry of Jilin University from 1997 to 1999. He joined the research group of Prof. V.W.W. Yam as a research assistant at Department of Chemistry of Hong Kong University in February 2000. He has been an associate professor since 1999 at NNU and a professor since 2003 at CIOMP of CAS. His current

research interests are the study of application of transition metal complex as gas sensors, and the organic light emitting devices (OLED).

Bingfu Lei received his BSc in 2001 in Food and Science Engineering and MSc in 2004 in inorganic chemistry from Jinan University, and then he began his PhD student experience under the supervising of Prof. Bin LI since 2004. His research interests mainly focuses on the study of exploration of covalently grafted hybrid as gas sensors, chemisensors and high luminescent display devices. He also interests in the research of afterglow phosphors based on impurity-doped inorganic materials.

Wenlian Li received his BSc degree in physics in 1967 from Jilin University, Changchun, China. He has been a professor at the CIOMP of CAS since 1995. He has been working on the topics including luminescence materials, device design and the design physics of OLED.

Shaozhe Lu received her BSc degree in solid luminescence in 1980 from University of Science and Technology, Hefei, China. She has been a researcher at the CIOMP of CAS since 2002. She has been working on luminescence materials, and analytical chemistry.